



Lateral Compression Properties of Special-Shaped 3D Tubular Woven Composites

Lihua Lyu, 0000-0002-7601-7509

Tingting Lyu, 0000-0002-1639-6607

Jingjing Wang, 0000-0002-8562-6285

Xiaoqing Xiong, 0000-0001-7790-4946

School of Textile and Material Engineering, Dalian Polytechnic University, Dalian 116034, P.R. China;

Corresponding Author: Lihua Lyu, lvlh@dpu.edu.cn

ABSTRACT

In order to avoid the instability of composite materials laminated tube connection between layer and layer, with green basalt fiber as raw material, through the reasonable design, the special-shaped 3D (three-dimensional) tubular woven fabrics with two different thicknesses and shapes were fabricated on a semi-automatic sample loom with low cost. The special-shaped 3D tubular woven composites were fabricated by VARTM (vacuum assisted resin transfer molding) process. The load-displacement curves and energy-displacement curves were obtained by lateral compression tests. The results showed that the same shape, the load and energy absorption values increased with thickness and compression property was better. For the special-shaped 3D tubular woven composites with the same thickness, the load and energy absorption values of the circular tube was larger than the square tube. The correlation coefficients of load-displacement and energy-displacement polynomial fitting formulas calculated by the least square method in the Origin 8.5 software were all close to 1, indicated that the fitting effect was good. This method provided a direction for the research of special-shaped 3D tubular woven composites.

1. INTRODUCTION

The 3D tubular composite is a kind of structural element with reasonable force form. Tubular composites are considered as lightweight advanced textile materials due to their advantages of high specific stiffness, high specific strength and good corrosion resistance [1]. Its applications are mainly concentrated in aerospace, pipeline transportation, transmission shaft, and various structural framework fields [2- 3]. Although 3D tubular composites have great application potential due to their excellent comprehensive properties, regular 3D tubular composites limit their application scopes. Because, circular tubular composite materials are greatly limited in complex environments, such as shaped tubes in the construction

field, shaped tubes heat exchangers in the mechanical field, nickel alloy special-shaped tubes etc. In the selection of these key components, circular tubular composite materials can not meet the requirements. Although the circular tubular composite is better at absorbing energy than the square tubular composite, the square tubular composite is easier to assemble with other components. Such as square fire valve, square door, unmanned chassis and so on. Square tube has irreplaceable advantages. Therefore, the development of special-shaped 3D tubular composites is more effective in adapting to the application of special structural composite in specific fields.

Generally, the tubular composite can be cured by laying-infiltration resin to form the two-dimensional laminated

ARTICLE HISTORY

Received: 22.08.2020

Accepted: 02.12.2021

KEYWORDS

3D woven fabric, special-shaped 3D tubular composites, failure mode, compression performance, fitting of a polynomial

To cite this article: Lyu L., Lyu T., Wang J., Xiong X. 2022. Lateral compression properties of special-shaped 3d tubular woven composites. *Tekstil ve Konfeksiyon*, 32(1), 77-85.

tubular composite. However, the fracture toughness of the two-dimensional laminated tubular composite is low, which resulted in the reduction of mechanical properties and integrity of the tubular composite. Compared with traditional tubular materials, 3D textile materials have advantages such as strong durability and can replace traditional materials [4]. Therefore, people began to prepare 3D tubular prefabricated parts based on techniques such as knitting and weaving, so as to obtain 3D tubular composite materials with stable mechanical properties. The weaving of 3D tubular woven fabric has been studied constantly by scholars. Tong et al. [5] analyzed the forming principle and interweaving rule of the zonal tubular fabric according to the structure of zonal tubular fabric and successfully produced it on an arrow loom, which provided corresponding technical support for the weaving of 3D tubular fabric. Wang [6] used the circular rail method to weave 3D tubular orthogonal woven fabrics. The paper carried out the numerical characterization of 3D tubular woven fabrics and established its geometric model to understand the mechanical properties of 3D tubular woven fabrics. These 3D looms or modified arrow looms can weave 3D tubular woven fabrics well, but the tension control of these looms was not stable and the moving parts of the looms were more, yarns were wasted in weaving. Gu [7] proposed a method for ordinary looms to weave 3D special-shaped fabric, that is the "flattening-weaving-reduction" method. After the weaving of 3D woven fabric was completed on ordinary looms, the 3D woven fabric can be formed by using the mould to support it when it is finished on the ordinary looms. This method made it possible to develop 3D woven composites at a low cost. Wang et al [8] used arylon fiber as raw material to prepare 3D woven tubular composites with different layers on sample looms by the "flattening-reduction" method. Wang et al. [9] successfully woven two kinds of special-shaped 3D tubular woven fabrics on the sample loom by designing reasonable structure diagrams. All the above researches provided the theoretical basis and the possibility of weaving for the low cost development of special-shaped 3D tubular woven fabrics on sample looms in this paper.

The mechanical properties of composite materials are the basis of their application in various fields. Therefore, the mechanical properties of composite materials such as tensile, bending, and compression, as well as failure modes and energy absorption are studied to reveal the structural characteristics of composite materials. Yan et al. [10] conducted an experimental study on the axial compression performance of a complete composite cylindrical shell, obtained the failure load of the cylindrical shell structure and load-strain curves of each measured point, concluded that the failure form of the structure was buckling failure. He et al [11] studied the torsional behavior of fiber reinforced composite tubes, analyzed the torsional damage, and established a single-cell model of the torsional damage mechanism of composite tubes to optimize the torsional properties of the yarn. Wu et al. [12] prepared a new 3D

multi-layered tubular braided composite material by combining knitting and weaving, studied its axial and radial compression performance. Found that the 3D braided tubular composite material showed better linear viscoelasticity when subjected to axial and radial compression. Zhu et al. [13] also analyzed the axial compression performance of 3D circular tubular woven composites through experiments and finite element simulation, The failure mode of the material was also analyzed through finite element method simulation in the paper, thus revealed the failure stress propagation, local stress concentration, and failure morphology of the material. It provided an effective reference for the design and application of 3D tubular woven composites. Palanivelu[14] studied the quasi-static compression performance and energy absorption of 9 kinds of composite tubes with different shapes, studied and compared the experimental parameters of these composite tubes, found that the specific energy absorption of special geometric shapes was higher than the standard or uniform cross section. Ma et al. [15] combined the respective advantages of circular pipe and square pipe, prepared circular - square shaped section composite pipe. By testing its energy absorption through quasi-static compression test. Well designed braided angle could be prepared circular - square shaped section composite pipe with high energy absorption performance. Chambe[16] conducted compression tests on several circular tubular composites with different materials and structures. The result showed that the unidirectional laminates with an orientation of 0° and stable braid layer achieved the expected energy dissipation. Most of the above researches on tubular woven fabric reinforced composites focused on regular 3D circular tubular woven composites, while few kinds of researches on special-shaped 3D tubular woven composites. Therefore, the development and preparation of a special-shaped 3D tubular composite will be an important research topic.

So far, the compression performance of 3D tubular composites has mainly focused on the axial compression test. There have been few reports on the lateral compression performance of 3D tubular composites. The lateral compression performance of special-shaped 3D tubular woven composites still needs to be further studied. Basalt fiber is characterized by high-temperature resistance, chemical corrosion resistance, high strength, and no pollution [17-18]. Therefore, this paper used high-performance basalt filament tow as raw to weave special-shaped 3D circular tubular and special-shaped 3D square tubular woven fabrics of different thicknesses on semi-automatic sample loom. Then the composite materials were made through VARTM. The lateral compression tests of special-shaped 3D circular tubular composites and special-shaped 3D square tubular composites were carried out to compare the lateral compression performance of 3D tubular composites with different section shapes. Finally, the compression failure mode and mechanism of the samples were investigated.

2. EXPERIMENTAL

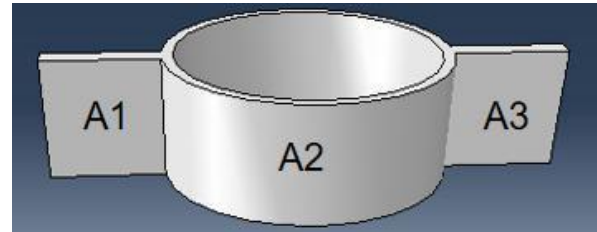
2.1 Materials and equipment

800 text basalt fiber filament tow (Zhejiang Shijin basalt fiber Co., Ltd.) was chosen as warp and weft yarn. Epoxy vinyl resin V-118 (Wuxi Qianguang Chemical Co., Ltd.) was used as a matrix. The SGA598 semi-automatic sample loom (Jiangyin Tongyuan Textile Machinery Co., Ltd.) was used for weaving samples, and the universal material testing machine (RGY-5 of Jiangsu Turbo Co., Ltd.) was used as the compression experiment instrument for the test.

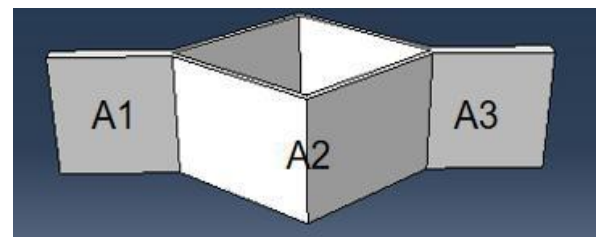
2.2 Design of special 3D tubular woven fabric

In the weaving process, double-grain plates were used to weave special-shaped 3D tubular woven fabrics by flat-circular tube-flat and flat- square tube-flat with different thicknesses. The weaving sketch of special-shaped 3D tubular woven fabric was shown in Figure 1 (a) and (b). A1 and A3 were the same plates, using the same radial section diagram. A2 adopted another grain plate, corresponding to another radial section diagram. In this paper, for the purpose of the comparative experiment, special-shaped 3D circular tubular and square tubular woven fabrics with a plate thickness of 2mm, number of heald frames of 4 and plate thickness of 4mm, number of heald frames of 8 were woven respectively. The relationship of thickness was $A1=A3=2A2$, The wall thickness of special-shaped 3D circular tubular woven fabric was the same as that of special-shaped 3D square tubular woven fabric, with the same radial section as shown in Figure. 2 and 3. In Figure 2

and 3, (a) is the warp structural drawing of A1 and A3 and (b) is the warp structural drawing of A2. According to the warp structural drawing. The chain drafts of special-shaped 3D tubular woven fabrics were drawn as shown in Figure.4 and 5. In Figure 4 and 5, (a) is the chain drafts of A1 and A3 and (b) is the chain drafts of A2.

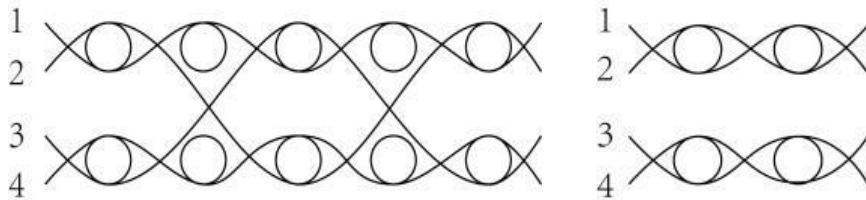


(a) Specific weaving sketch of special-shaped 3D circular tubular woven fabric



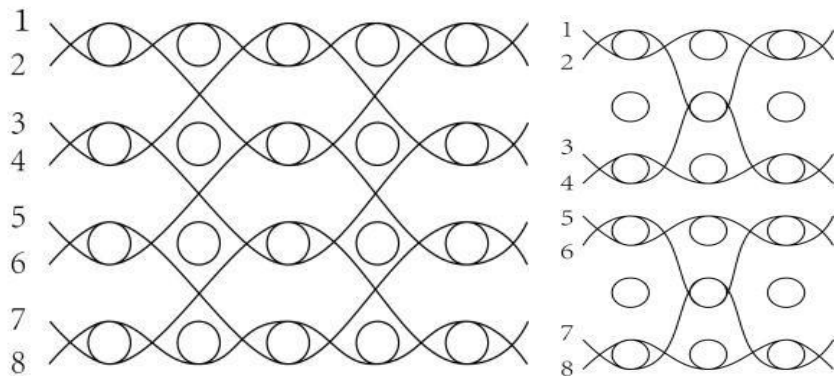
(b) Specific weaving sketch of special-shaped 3D square tubular woven fabric

Figure 1. Specific weaving sketch of special-shaped 3D tubular woven fabric



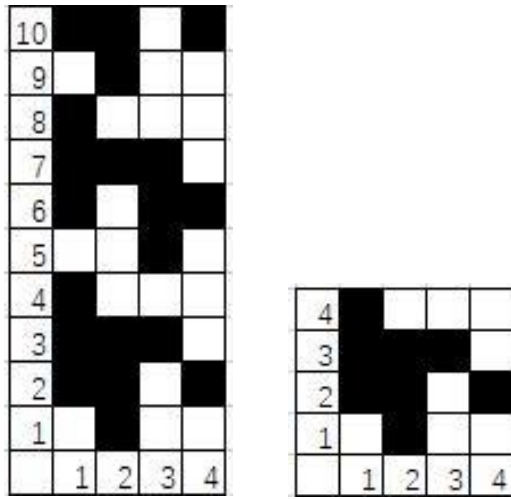
(a) Warp structural drawings of A1 or A3 (b) Warp structural drawings of A2

Figure 2. Warp structural drawings of special-shaped 3D tubular woven fabrics with the thickness of 1mm



(a) Warp structural drawings of A1 or A3 (b) Warp structural drawings of A2

Figure 3. Warp structural drawings of special-shaped 3D tubular woven fabrics with the thickness of 2mm

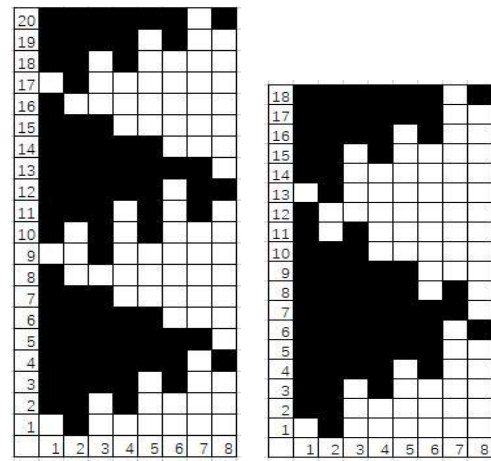


(a) Chain drafts of A1 or A3 (b) Chain drafts of A2

Figure 4. Chain drafts of special-shaped 3D tubular woven fabrics with the thickness of 1mm

2.3 Woven of Special-Shaped 3d Tubular Woven Fabric

800 text basalt fiber filaments tows was chosen as warp and weft yarn. Reed of 40 (40 teeth /10 cm) was used on SGA598 semi-automatic small sample loom, with 4 or 8 sleys per reed to pass through the basalt fiber yarn. The width of 15cm, the wall thickness of 2 mm which the total number of roots was 240 and that of 4 mm wall thickness was 480. The weaving parameters of the special-shaped 3D tubular woven fabric are given in Table1.



(a) Chain drafts of A1 or A3 (b) Chain drafts of A2

Figure 5. Chain drafts of special-shaped 3D tubular woven fabrics with the thickness of 2mm

2.4 Preparation of Special-Shaped 3d Tubular Composites

The special-shaped 3D tubular woven fabric strengthens the body, with epoxy vinyl resin as the matrix was compounded by the VARTM molding process. Among them, The epoxy is V-118, the curing agent was methyl ethyl ketone peroxide, the accelerant was cobalt octoate. The volume ratio of resin, curing agent, and accelerator was: V resin: V curing agent: V accelerator =100:3:3. The VARTM molding process diagram of a special-shaped 3D tubular woven composite is shown in Figure. 6.

Table 1. Weaving parameters of special-shaped 3D tubular woven fabrics of different thicknesses

Partition thickness (mm)	Wall thickness (mm)	The layer number of yarns		Warp density (threads/10cm)	Weft density (threads/10cm)
		A1、A3、	A2		
2	1	2	1	160	50
4	2	4	3	320	50

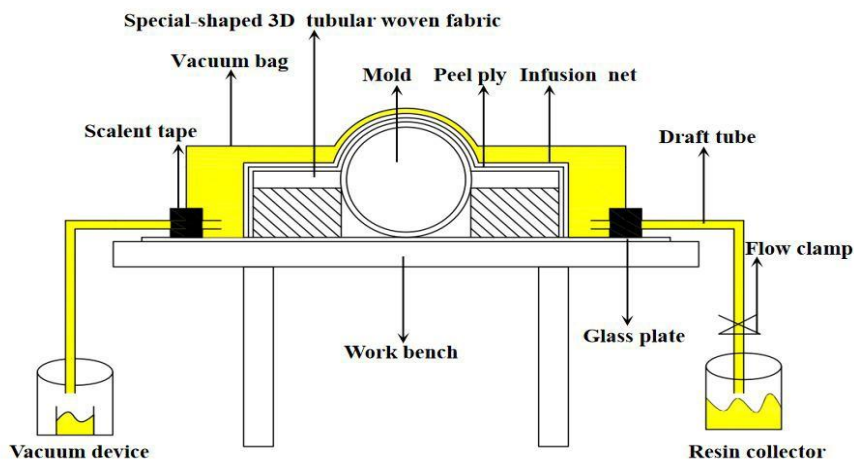


Figure 6. VARTM molding process diagram of special-shaped 3D tubular woven composite material

3. COMPRESSION PERFORMANCE TEST

The test of lateral compression was conducted according to fiber-reinforced thermosetting plastic composites pipe-determination for external loading properties by parallel-plate loading (GB/T5352-2005). The special-shaped 3D tubular woven composites were prepared with a height of 30mm and a width of 90mm samples. The compression properties of the four samples were tested under the same experimental conditions. In the universal testing machine (RGY-5) compression test, the testing speed was 10mm/min. The data obtained through the compression experiment was plotted in Origin 8.5 to obtain the load-displacement curve and energy-displacement curves.

4. RESULTS AND DISCUSSION

4.1 Load-Displacement Curve and Fitting Value

In this paper, the lateral compression performance of special-shaped 3D tubular composites was evaluated and analyzed employing load-displacement curves and energy-displacement curves. The fitting curve of load-displacement was obtained by 8-orders polynomial fitting method. Two kinds of different thicknesses and different shapes of special-shaped 3D tubular woven composites load-displacement curves and fitting curves were shown in Figure 7. According to load-displacement fitting curves, the mathematical equation of fitting curve and correlation coefficient between displacement and load can be obtained, as shown in Table 2. The results of fitting curves were related to the correlation coefficient R, whose value ranged from 0 to 1 and was infinitely close to 1. If the value of R was closer to 1, the simulation results will be better.

In Figure 7, the maximum load of special-shaped 3D tubular composites of the same shape increased with the increase of thickness. It can be seen that the thickness of both special-shaped 3D circular tubular composites and special-shaped 3D square tubular composites has a relatively large impact on the load. A load of special-shaped 3D tubular composite with the thickness of 1mm increased continuously with the increase of displacement. This was mainly due to the special-shaped 3D tubular composite material under lateral compression was wall bearing, but the thinner wall can beared less load. In the compression process, its elastic linearity was good, so the load increased with the increase of displacement. The load-displacement curve for 2 mm special-shaped 3D

tubular composites was divided into three stages. In the first stage, the fitting curves were almost linear, which showed linear elastic properties before the load was reached its peak, this indicated that the bonding situation was relatively good between resin and fiber. The overall force made the special-shaped 3D tubular composite surface without damage. In the second stage, the slope of the curve decreased with the increase of displacement, This was because the contact surface area increased with the increase of displacement between the samples and indenter, and the resin began to destroy. After the resin cracked, the reinforced fiber gradually cracked under force until the load reached the peak, the special-shaped 3D tubular composite began to have the overall failure. In the third stage, the curve began to decline. At this point, the special-shaped 3D tubular composite began to have shear destruction, but the fiber without fracture could be born a part of the load, so the load gradually decreased with the increase of displacement. At the initial stage, with the gradual increase of the load, the special-shaped 3D tubular composite deformed elastically. In the elastic region, the composite presented linear strain due to the initial stress action. The second stage corresponds to plastic deformation, in which fibers and resins were continuously compressed and the stress increased with the strain during compression. Finally, the overall failure of the material occurred after the stress reached the peak.

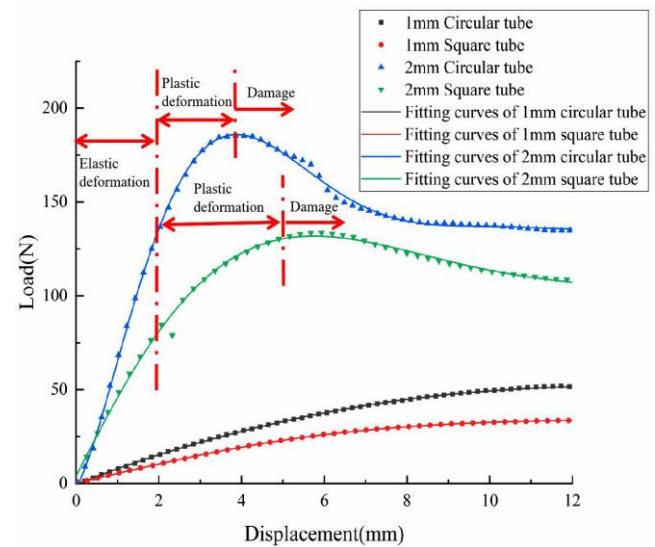


Figure 7. Load-displacement scatter plots and fitting curves of two 3D tubular woven composites with different thicknesses and different shapes

Table 2. Mathematical equation of fitting curve and correlation coefficient of load-displacement relationship

Thicknesses/m	Mathematical model equation of fitting curve	Correlation coefficient
1mm Circular tube	$Y=-0.707+9.279x-0.808x^2+0.108x^3-0.013x^4+8.152\times 10^{-4}x^5-2.519\times 10^6x^6+3.405\times 10^{-7}x^7-1.202\times 10^{-9}x^8$	0.9997
1mm Square tube	$Y=-0.368+4.810x+0.282x^2-0.107x^3+0.009x^4-4.722\times 10^{-4}x^5+1.256\times 10^{-5}x^6-1.774\times 10^{-7}x^7+1.044\times 10^{-9}x^8$	0.9998
2mm Circular tube	$Y=-4.072+42.937x+0.172x^2-1.655x^3+0.260x^4-0.019x^5+7.110\times 10^{-4}x^6-1.409\times 10^{-5}x^7+1.141\times 10^{-7}x^8$	0.9998

Because the stress of the special-shaped 3D square tubular composite was mainly concentrated at the compression point during the compression process, the load-displacement curve gradually increased.

In general, The trend of load-displacement curves of special-shaped 3D tubular composites varied with different thicknesses. The load displacement curve of 1mm special-shaped 3D tubular composite material showed a trend of gradually increasing, while that of 2mm special-shaped 3D tubular composite material showed a trend of first increasing and then decreasing. The bearing capacity of the same tube wall shape increased with the increase of thickness, which indicated that the special-shaped 3D tubular composite with larger thickness has greater rigidity. From the correlation coefficient in Table 2, the correlation coefficient R of the four curves were all greater than 0.99, so it could be seen that there was a high correlation between them, indicated that the fitting curve and the actual curve have a good consistency. The least square fitting can well describe the relationship between load and displacement.

4.2 Energy-Displacement Curve and Fitting Value

Energy absorption of the composite was a special requirement of mechanical properties, which can be used to measure the mechanical properties of composites. Through the compression test, the energy-displacement curve of the composite was obtained by integrating the compression load of the composite with the mathematical integration method. Figure 8 showed the energy-displacement curve of the special-shaped 3D tubular composite with different thicknesses and shapes. According to the energy-displacement fitting curves, the mathematical model equation of fitting curve and correlation coefficient of energy-displacement relationship was shown in Table 3.

It could be clearly seen from Figure 8 that the energy absorption by the material under the action of load gradually increased with the increase of displacement. Under the same thickness, the energy absorption value of special-shaped 3D circular tubular woven composites was greater than that of special-shaped 3D square tubular woven composites, which indicated that the impact resistance of special-shaped 3D circular tubular woven composites was better than that of special-shaped 3D square tubular woven composites. However, under the same shape, the energy

absorption value of special-shaped 3D tubular woven composites increased with the increase of thickness under the same displacement, which also indicated that the buffering and impact resistance of special-shaped 3D tubular woven composites increased with the increase of pipe wall thickness. According to the correlation coefficient in Table 3, the correlation coefficients of the four curves were all greater than 0.99 and close to 1, so the fitting effect was good. The failure modes of the two special-shaped 3D tubular woven composites were the same, which mainly shear failure. First, at the beginning of compression, there was no obvious damage on the surface of the material, and the energy absorption curve increased linearly. With the further increased of load, the slope of energy-displacement curve decreased gradually. At this time, the fiber bundle gradually flexed in some areas, which lead to the gradual separation of the fiber from the surrounding matrix until the overall failure of the material.

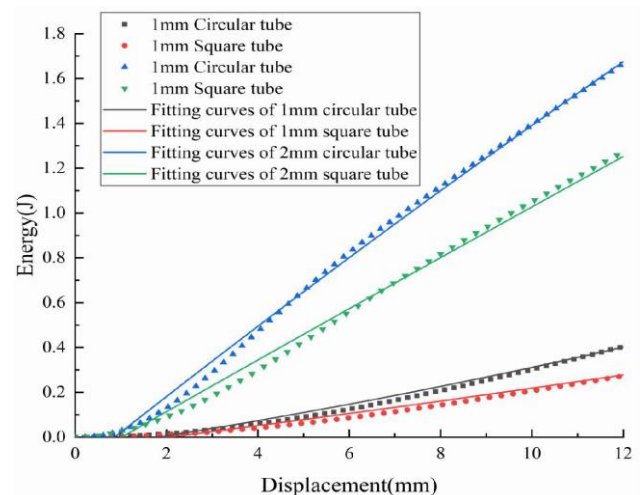


Figure 8. Energy-displacement scatter plots and fitting curves of two 3D tubular woven composites with different thicknesses and different shapes

4.3 Compression Failure Process and Failure Mode

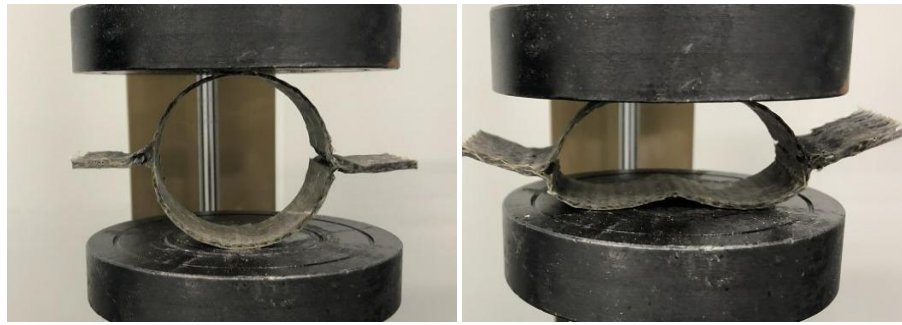
4.3.1 Compression failure process

Failure mechanism was an important index for evaluating the compression performance of energy-absorbing structures of composite materials. The failure process of special-shaped 3D tubular composites was shown in Figure 9. (a) was the compression process of 1mm thick special-shaped 3D circular tubular composite material, (b) was the

Table 3. Mathematical equation of fitting curve and correlation coefficient of energy-displacement relationship

Thicknesses (mm)	Mathematical model equation of fitting curve	Correlation coefficient
1mm Circular tube	$Y=-9.862+9.611x+2.137x^2$	0.999
1mm Square tube	$Y=-7.605+7.412x+1.381x^2$	0.998

2mm Circular tube	$Y=-134.081+158.641x-0.553x^2$	0.996
2mm Square tube	$Y=-81.255+94.241x+1.835x^2$	0.996



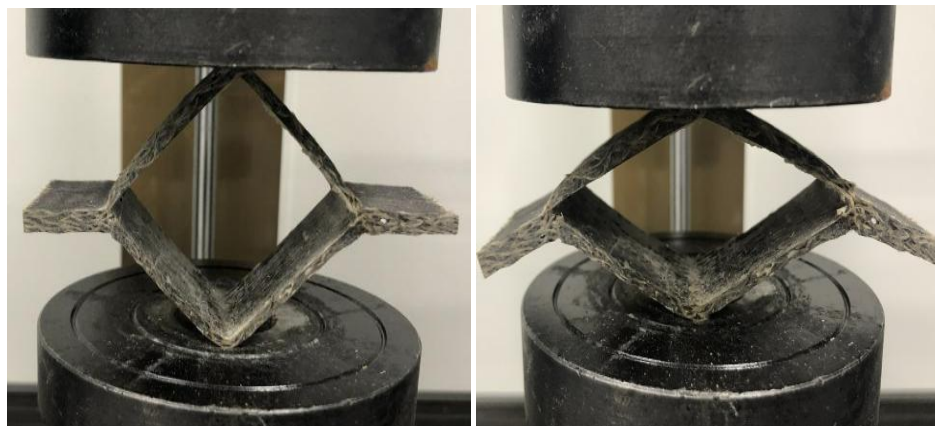
(a) Special-shaped 3D circular tube composite material compression process of 1 mm



(b) Special-shaped 3D circular tube composite material compression process of 2 mm



(c) Special-shaped 3D square tube composite material compression process of 1mm



(d) Special-shaped 3D square tube composite material compression process of 2 mm

Figure 9. Compression process of 3D tubular composites with different thicknesses

compression process of 2 mm thick special-shaped 3D circular tubular composite material, (c) was the

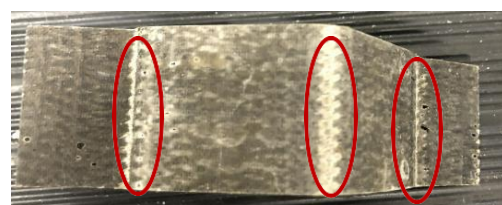
compression process of 1mm thick special-shaped 3D square tubular composite material, and (d) was the

compression process of 2 mm thick special-shaped 3D square tubular composite material. The lateral pressure process of special-shaped 3D tubular composite material could be roughly divided into three stages: elastic deformation stage, plastic deformation stage, and inner wall contact stage. In order to ensure equipment's safety in the experimental process, this stage should be avoided. Under the lateral compression, the wings A1 and A3 zones of the special-shaped 3D tubular composite without any role, and only the tubular part A2 zone suffered shear destruction. The contact between the special-shaped 3D circular tubular composite material and the upper and lower two steel plates of the universal testing machine was mainly concentrated at two points at the end of the vertical diameter of the tube. At this time, the compression was just beginning, the tubular part showed an arc of elastic deformation. As the upper steel plate continued to drop, the special-shaped 3D tubular woven composite reached its peak load. At this time, the fibers in the special-shaped 3D tubular composites began to crack gradually, after some fibers were broken and the peak load dropped until all of them were broken. The vertical ends of the special-shaped 3D square tubular composite contacted with the pressing plate at first, and the tubular part was transversely deformed and longitudinally compressed. As the load increased gradually, the fiber fracture occurred gradually at the connection between both sides of the square pipe and the two wings.

4.3.2 Compression failure mode and mechanism

Special-shaped 3D tubular composites were mainly caused by pipe wall fracture failure. Although the wings do not play a supporting role in lateral compression, the load was

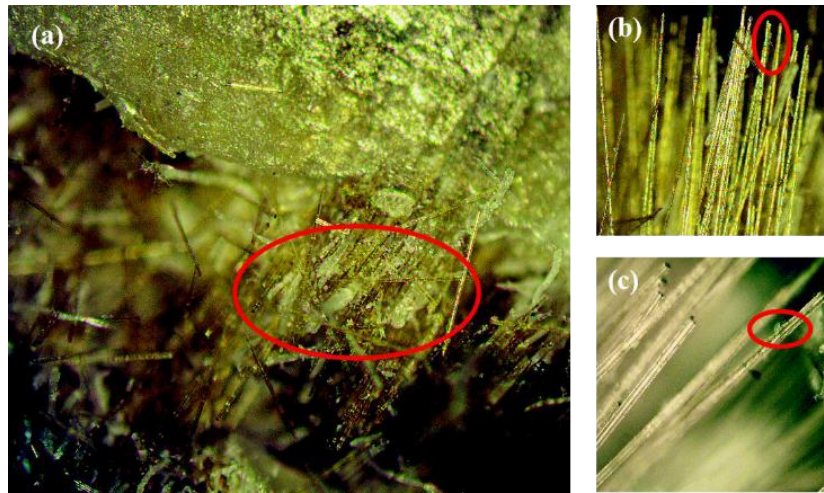
transferred to the sidewall of the pipe during compression, resulted in bending and buckling at the connection between the pipe and the two wings to form a plastic fracture. At the beginning of compression, the contact area between the pressure plate and the pipe wall was small, it was only concentrated at the end of the vertical diameter of the pipe. At this time, the load on the pipe wall was small. With the pressing plate exerted pressure on the pipe wall gradually, the compression load increased linearly with the increase of displacement until it reached the maximum load, the resin matrix on the surface of the tubular composite first produced longitudinal extension crack and the matrix cracked, then the outermost reinforcement fiber connected with the resin matrix break firstly. As other fibers without fracture provided some resistance, the compression load decreased gradually after reaching the peak value. Finally, the pipe wall was almost completely compressed laterally, the fiber was completely broken, the vertical diameter of the pipe and the area where the pipe wall was connected with the two wings were bent and broken. The failure pattern was shown in Figure 10 (a) and (b). In general, the compressive failure modes of the special-shaped 3D tubular composites were fiber brittle fracture and pulling, matrix cracking and typical shear failure, but there was no lamination, and the overall performance was still good. As can be seen from the optical microscope image of the failure mode of the special-shaped 3D tubular composites in Figure. 11. There were a large number of fiber fracture and pulling in the damaged part of the material. And it can be seen from the local magnification that the resin was broken when the material was damaged.



(a) Failure modes of special-shaped 3D circular tubular woven composites

(b) Failure modes of special-shaped 3D square tubular woven composites

Figure 10. Failure modes of special-shaped 3D tubular woven composites



(a) Overall optical microscope image of the damage pattern (b) and (c) Local magnified image
Figure 11. Optical microscope image of failure modes of special-shaped 3D tubular woven composites

5. CONCLUSION

Two kinds of special-shaped 3D tubular woven fabrics of different thicknesses and shapes were woven on an ordinary loom by reasonable design with low cost processing. The special-shaped 3D tubular woven fabrics acted as reinforcement, and at the same time, epoxy vinyl resin was used as a basal body by the VARTM molding process to produce special-shaped 3D tubular woven composite materials and tested their lateral compression performance. In origin 8.5 software used the least squares fitting of the data, draw load- displacement scatter plots and fitting curves and energy-displacement scatter plots and fitting curves. Results showed that the thickness was 2 mm of the special-shaped 3D circular tubular woven composites have the greatest load and energy absorption value, the thickness was 2mm of the special-shaped 3D square tubular woven composite load and energy absorption value of the second, and then the thickness was 1mm of special-shaped 3D circular tubular woven composite material, load, and energy absorption of the minimum value was 1 mm of the special-shaped 3D square tubular woven composite. In addition, the polynomial fitting curves were basically concerned with the

experimental scatter plots, which proved the accuracy of the quasi-determination of the polynomial fitting. In the right model curve analysis of two different thicknesses under different shapes special-shaped 3D tubular woven composites failure process and failure mode. The special-shaped 3D tubular woven composites compression failure characterized by shear failure mode and special- shaped 3D tubular woven composites for the overall destruction did not appear the phenomenon of layering, indicated that special-shaped 3D tubular woven composites have excellent mechanical properties. The compression performance of special-shaped 3D tubular woven composites was greatly different with different wall shapes and thicknesses, but the compression process and compression failure mechanism were the same.

Acknowledgement

This research was funded by the National Science Foundation of Liaoning Province (2019-MS-017) and Technological Innovation Team Project of Liaoning Province (LT2017017).

REFERENCES

1. Ma WS, Ma ZY, Ren BJ, Fan WF. 2017. Meso-structure and modeling of a new three-dimensional braided tubular material. *Journal of Reinforced Plastics and Composites*, 37(5), 310-320.
2. Zhong WX, Sun XL, Ma PB. 2015. Application and development of tubular composites. *Fiber Glass*, 000(001), 47-52.
3. Luo SH, Yang CY. 2015. Research progress on the mechanical properties of tubular composite. *Technical Textiles*, 33(08), 1-5.
4. Bharti K, Kumaraswamidhas LA, Das RR. 2020. Detailed investigation of adhesive fillet tubular T-joint of laminated FRP composite tube under axial compressive load. *Welding in the World*, 64(7), 1279-1292.
5. Tong Y. 2016. Design and production of partial warp tubular fabric. *Cotton Textile Technology*, 44(08), 71-74.
6. Wang W, Zhu JH, Zhang RY, Li YL, Ji F, Yu JY. 2018. Numerical characterization and simulation of the three-dimensional tubular woven fabric. *Journal of Industrial Textiles*, 47(8), 2112-2127.
7. Gu P. 2002. A new weaving technique of 3-dimensional preforms for composites by conventional loom. *Journal of Textile Research*, (05), 24- 26+2.
8. Wang LL, Xu AC, Zhang SY. 2017. Study on tensile mechanical properties of three-dimensional tubular composites. *Journal of Wuhan Textile University*, 30(03), 12-16.
9. Wang GJ, Wang JJ, Lyu LH. 2019. Design and trial weaving of two abnormal 3d tubular woven fabric. *Cotton Textile Technology*, 47(05), 64-67.
10. Yan G, Han XJ, Yan CL, Zuo CC, Cheng XQ. 2014. Buckling analysis of composite cylindrical shell under axial compression load. *Acta Materiae Compositae Sinica*, 31(03), 781-787.
11. He B, Mi ZX, Wang YJ, Gu BH. 2019. Unit cell modeling on torsion damage behavior of a novel three-dimensional integrated multilayer fabric-reinforced composite tubular structure. *Textile Research Journal*, 89(19-20), 4253-4264.

-
12. Wu T, Cao HJ, Qian K, Luo BR. 2012. Preparation and compression properties of new three-dimensional multi-layer tubular braided composites. *Fiber Reinforced Plastics/Composites*, (03), 19-22.
 13. Zhu LM, Zhang HW, Guo J, Wang Y, Lyu LH. 2020. Axial compression experiments and finite element analysis of basalt fiber/epoxy resin three-dimensional tubular woven composites. *Materials*, 13(11),2584.
 14. Palanivelu S, Paeppegem WV, Degrieck J, Kakogiannis D, Ackeren JV, Hemelrijck DV, Wastiels J, Vantomme J. 2010. Comparative study of the quasi-static energy absorption of small-scale composite tubes with different geometrical shapes for use in sacrificial cladding structures. *Polymer Testing*, 29(3), 381-396.
 15. Ma Y, Yang YQ. 2015. Energy absorption mechanism of circular-square irregular section composite tubes. *Acta Materiae Compositae Sinica*, 32(01), 243-249.
 16. Chambe JE, Bouvet C, Dorival O, Ferrero JF. 2020. Energy absorption capacity of composite thin-wall circular tubes under axial crushing with different trigger initiations. *Journal of Composite Materials*, 54(10), 1281-1304.
 17. Zheng ZC, Ge LH, Chen Y, Sun SY, Wang Q. 2011. Research on mechanical properties of continuous basalt fiber reinforced resin composites. *Aeronautical Manufacturing Technology*, (17), 66-68+72.
 18. Bu FQ, Dong Y, Jin WG, Zhang WZ, Du XG. 2019. Characteristics and application of basalt fiber composites. *Brand & Standardization*, (03), 56-58+61.